

Simulation Study on the Influence of High Toroidal Mode Number $n=4$ RMP Phases on Plasma Response

Lingjie Zhou¹, X.J. Zha²

¹(College of Science, Donghua University, Shanghai, China

Email: 819201412@qq.com)

¹(College of Science, Donghua University, Shanghai, China

Email: xjzha@dhu.edu.cn)

Abstract:

Abstract: Based on the equilibrium constructed from the EAST device discharge 115766, this study employed a linear plasma response model computed with the MARS-F program to investigate the influence of different RMP coil phase angles, under conditions of equal RMP coil current and zero phase difference. Simulation results indicate that the deformation of the plasma, under the influence of RMP fields, occurs only within a thin layer at the plasma boundary, manifesting a typical edge-peeling-like response. Notably, the plasma response at an RMP phase angle of 180° was more pronounced than at 0° , demonstrating that even with the same phase difference, different RMP phase angles can lead to significant variations in plasma response. This study provides crucial theoretical guidance for the design of RMP coil currents and their application in controlling Edge Localized Modes (ELMs) experiments.

Keywords — Plasma Responses, MARS-F code, Resonant Magnetic Perturbation, RMP phase.

I. INTRODUCTION

When tokamak devices operate in high confinement mode (H-mode), Edge Localized Modes (ELMs) periodically occur in the boundary plasma regions [1]. ELMs pose potential threat for future tokamak devices such as the International Thermonuclear Experimental Reactor, ITER, as each ELMs event results in a rapid outward transport of a significant amount of plasma particles and energy from the core area, which eventually impacts the surfaces of plasma-facing components (PFCs) [2]. These transient high particle and heat fluxes can shorten the lifespan of PFCs. Currently, the effectiveness of externally applied resonant magnetic perturbation (RMP) fields in controlling ELMs has been demonstrated through numerical simulations and experiments across many tokamak devices [3-8]. Present research indicates that the process of controlling ELMs with RMP fields is associated with the plasma response [9]. In ITER and other advanced tokamak devices, compared to low-mode-number ($n=1$ and $n=2$) RMPs, high-mode-number ($n=3$ and $n=4$) RMPs have a lesser impact on the confinement of plasma particles and

energy [10]. Therefore, this study employs $n=4$ RMP coils.

A typical RMP ELM discharge 115766 from EAST device is chosen for the starting equilibrium in this work. During this discharge, the RMP fields are consistent across different times; however, the phase angle of the RMP field does affect the plasma response.

The linear plasma response model developed using the MARS-F [11] code has successfully integrated a self-consistent plasma response into the computational models and has been extensively applied for theoretical and numerical simulation studies across multiple tokamak devices.

II. BASED ON THE EAST DEVICE DISCHARGE, EQUILIBRIUM AND CORRESPONDING RMP COIL MODELS WERE CONSTRUCTED.

For the EAST device discharge number 115766, equilibria are constructed based on experimental data at two time points: 3.45s, and 3.73s. At 3.45s and 3.73s, RMP coil currents were introduced with phases of 180° and 0° , respectively. It is important

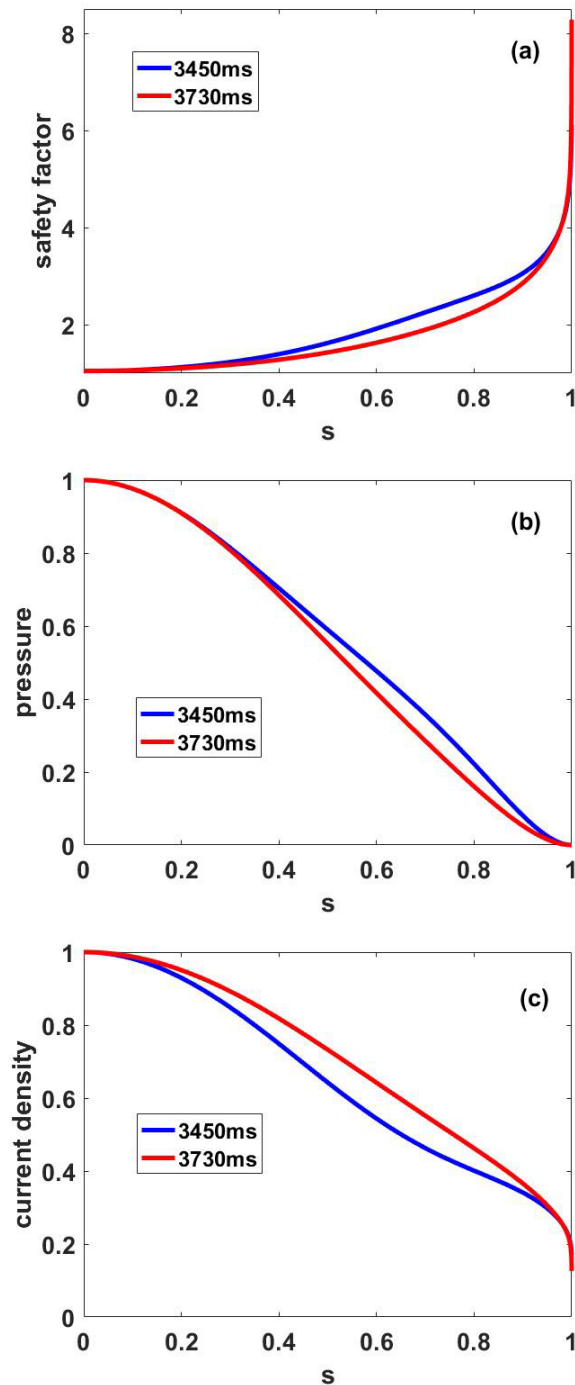
to note that at both time points, the phase difference between the upper and lower groups of RMP coil currents was 0° , i.e., $\Delta\phi = \phi_U - \phi_L = 0^\circ$, and the amplitude of the coil currents was the same at 14 kAt. In other words, the considered RMP fields at 3.45s and 3.73s only differ in their toroidal angle.

Figure 1 provides a comparison of the equilibrium configurations at the three time points, where the key equilibrium parameters (Table 1) are: q_0 , q_{95} , q_a and β_N , with q_0 being the safety factor on the magnetic axis, q_{95} safety factor at 95% normalized poloidal flux q_a the safety factor on the plasma edge and $\beta_N \equiv \beta(\%)a(m)B_0(T)/I_p(MA)$, with β being the plasma volume averaged pressure normalized by the magnetic pressure, and a the plasma minor radius, B_0 the toroidal vacuum field at plasma major radius R_0 and I_p the total plasma current. Figure 1(a-c) compares the radial distribution of the safety factor, plasma equilibrium pressure and plasma current density. The plasma boundary shape for this equilibrium with minor radius $a = 0.45m$ and major radius $R_0 = 1.75m$. Noted that due to numerical reasons, the plasma boundary near the X-point has been smoothed. However, studies indicate that minor smoothing at the position of the X-point has little effect on the plasma response [12].

Figure 1(d) shows the geometric distribution of the RMP coils in the poloidal cross-section, with positions on the (R, Z) plane from top to bottom listed as (2.092, 0.759), (2.278, 0.577), (2.278, -0.577), and (2.092, -0.759) in meters. In the EAST device, there are two sets of coils, each consisting of eight coils with four turns per coil. During discharge number 115766, a toroidal mode number $n=4$ was employed for the RMP coil current configuration, rendering the RMP field during this discharge as a static field.

Table 1 the equilibrium data at the time points 3.45s, and 3.73s.

time slice #	q_0	q_{95}	q_a	β_N
3.45s	1.043	3.927	6.127	1.393
3.73s	1.045	3.917	7.584	1.285



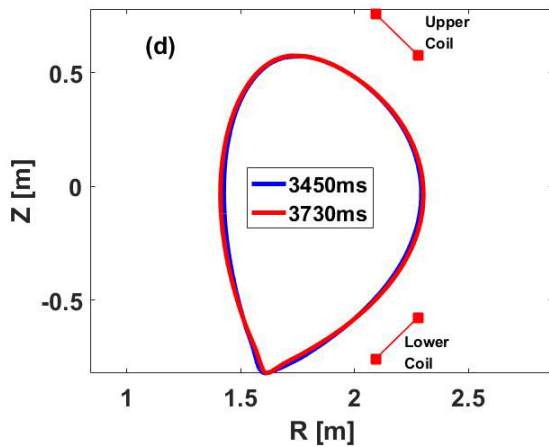


Fig.1 Based on discharge 115766 on EAST at 3.45s and 3.73s time slices, comparison of (a)the radial profiles of the safety factor, (b) the plasma equilibrium pressure, (c) plasma current density and (d) the poloidal cross-section of the plasma boundary and the location of RMP coils (red-square). Here the blue-solid and red-solid curves denote the 3.45s and 3.73s. And $s \equiv \psi_p$, ψ_p represents the normalized equilibrium poloidal magnetic flux.

III. PLASMA RESPONSE MODEL

A linear plasma response model is constructed using the MARS-F code, a linear single-fluid magneto-hydrodynamic (MHD)program designed for toroidal geometry configurations, which simulates the plasma response induced by the RMP field. The required plasma equilibrium for MARS-F is provided by solving the fixed boundary Grad-Shafranov equation using the CHEASE program.

In this study, the response of the plasma to a toroidal mode number $n=4$ RMP field was analyzed using the MARS-F program. This program describes the dynamics under toroidal geometry using a set of linearized single-fluid MHD equations that incorporate resistivity and plasma rotation, as indicated in equations (1) through (5):

$$i(\Omega_{RMP} + n\Omega)\xi = v + (\xi \cdot \nabla\Omega)R\hat{\phi} \quad (1)$$

$$i\rho(\Omega_{RMP} + n\Omega)v = -\nabla p + j \times B + J \times b - \rho[2\Omega\hat{z} \times v + (v + (v \cdot \nabla\Omega)R\hat{\phi})] \quad (2)$$

$$i(\Omega_{RMP} + n\Omega)b = \nabla \times (v \times B - \eta j) + (b \times \nabla\Omega)R\hat{\phi} \quad (3)$$

$$i(\Omega_{RMP} + n\Omega)\rho = -v \cdot \nabla P - \Gamma P \nabla \cdot v \quad (4)$$

$$j = \nabla \times b, \quad (5)$$

Where Ω_{RMP} represents the frequency of the externally applied resonant magnetic perturbation coil current. $n\Omega$ represents the Doppler frequency shift, Ω is the angular frequency of the toroidal rotation of the plasma. ξ , v , j , b and p are the plasma displacement, the perturbed velocity, current, magnetic field and pressure, respectively. And ρ , B , J and P denote the equilibrium density, magnetic field, current and pressure. R is the major radius of the plasma, \hat{z} and $\hat{\phi}$ are the unit vector in the vertical direction within the poloidal plane and the unit vector in the geometric toroidal angle direction, respectively. η represents the resistivity of the plasma, and $\Gamma = 5/3$ is the adiabatic index for an ideal gas.

IV. THE PLASMA RESPONSE TO N=4 RMP FIELD

Using the linear magneto-hydrodynamic program MARS-F [11], a linear plasma response model was constructed to calculate the plasma response to an $n=4$ toroidal mode number RMP field at two equilibrium times during the discharge. The simulation results are displayed in figure 2 and figure 3.

Figure 2(a-b) presents the distribution of the perturbed magnetic field in the poloidal cross-section at times 3.45s and 3.73s, considering RMP fields at 180° and 0° , respectively. The results indicate a notable plasma response at the plasma boundary at 3.45s; whereas at 3.73s, with the 0° RMP field, the response is confined primarily near the rational surfaces, predominantly characterized by shielding effects at the plasma boundary. Despite the zero phase difference between the upper and lower coil sets at both timestamps, the plasma response varies significantly with the phase angle of the RMP field. This demonstrates that the phase angle of the RMP field crucially influences the plasma response, even when other parameters such as coil configuration remain constant.

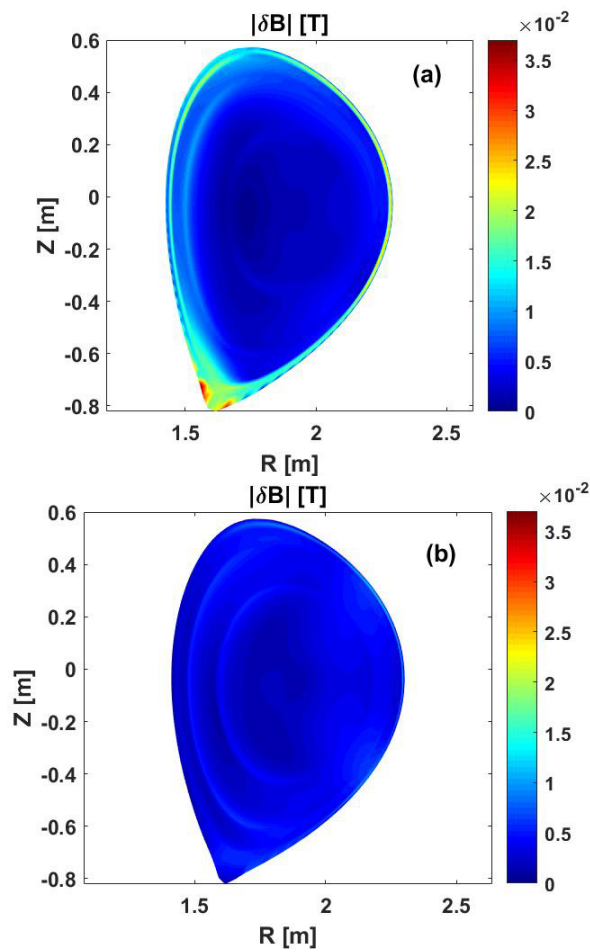


Fig.2 The plasma response to $n=4$ RMP field. Figures (a-b) display the amplitude of the perturbed magnetic field $|\delta B|$. Here figure (a) corresponds to the 3.45s moment with a 180° RMP coil current and (b) corresponds to the 3.73s moment with a 0° RMP coil current.

Figure 3(c-d) displays the distribution of the normal displacement in the poloidal cross-section at times 3.45s and 3.73s. At both timestamps, significant normal displacements are observed near the X-point, similar to the results shown in Figure 2(a-b). At 3.45s, under the 180° RMP coil current phase angle, the normal displacement perturbations near the X-point are larger. In conjunction with previous studies on plasma response [13-14], these results suggest that the plasma exhibits a stronger response to the $n=4$, 180° RMP field at 3.45s. This enhanced response is

indicative of the sensitivity of plasma behavior to the phase angle of the RMP field, especially in configurations involving complex interactions at rational surfaces.

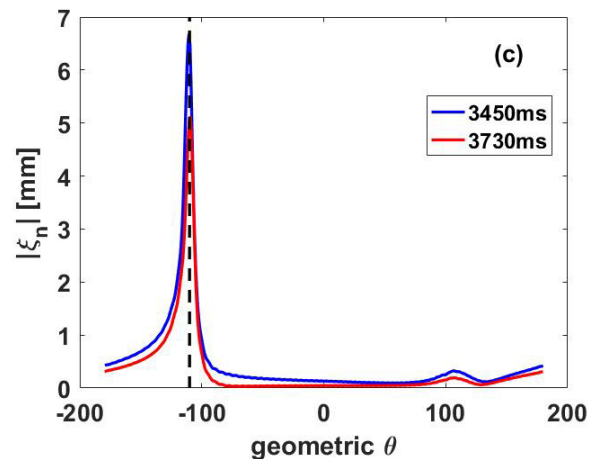
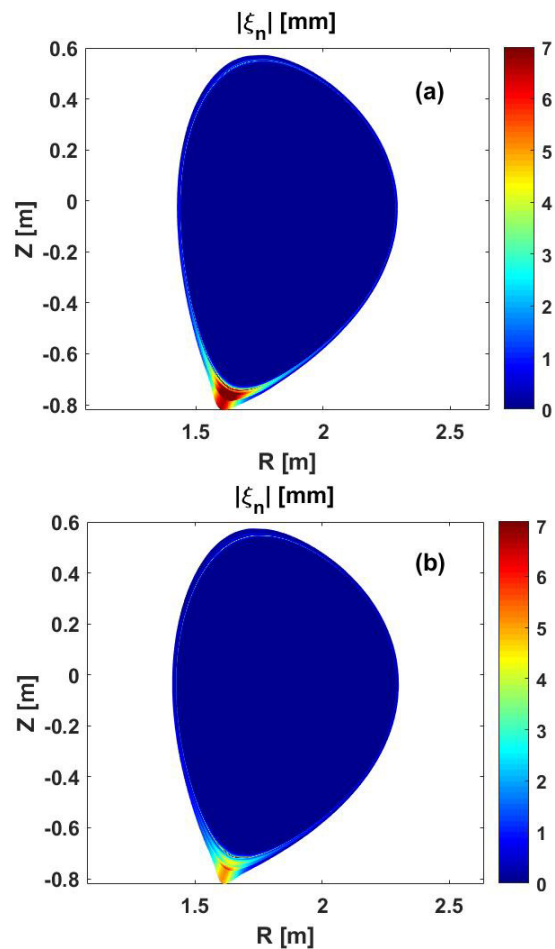


Fig.3 The plasma response to $n=4$ RMP field. Figures (a-b) show the amplitude of the normal displacement $|\xi_n|$ across the poloidal section,

where figure(a) corresponds to the 3.45s moment with a 180° RMP coil current and (b) corresponds to the 3.73s moment with a 0° RMP coil current. Figure(c) depicts the amplitude of the normal displacement of the plasma surface along the geometric poloidal angle, with $\theta = -110^\circ$ (black vertical dashed line) indicating the position of the X-point. Here the red-solid and blue-solid curves denote the 3.45s and 3.73s.

V. CONCLUSIONS

The plasma response to the Resonant Magnetic Perturbation field, related to the phase of the RMP coil current, is computed and analyzed utilizing the MARS-F code. Under the influence of RMP field, perturbations magnetic field perpendicular to the plasma surface and perturbation displacements perpendicular to the plasma surface are generated, leading to deformations at the plasma boundary. This study begins with a plasma equilibrium reconstructed from discharge 115766 of EAST device. The simulation results indicate that plasma deformation due to different RMP phase angles occurs only within a thin layer at the plasma boundary, characterizing the response as a typical boundary peeling-like response. Although the phase differences $\Delta\phi$ between the upper and lower RMP coils are zero and the coil currents are the same at both 3.45s and 3.73s, the plasma responses differ significantly due to the different RMP phase angles at these times (180° at 3.45s and 0° at 3.73s). Specifically, the plasma response at 3.45s with an RMP phase angle of 180° is stronger than at 3.73s with an RMP phase angle of 0° . This study provides crucial theoretical guidance for the design of RMP coil currents and their application in controlling ELMs experiments. The results obtained through simulations can be tested in future RMP experiments at the EAST device.

REFERENCES

- [1] Ren J, Liu Y, Liu Y, et al. Feedback stabilization of ideal kink and resistive wall modes in tokamak plasmas with negative triangularity[J]. Nuclear Fusion, 2018, 58(12): 126017.
- [2] Leonard A W. Edge-localized-modes in tokamaks[J]. Physics of Plasmas, 2014, 21(9).
- [3] Suttrop W, Eich T, Fuchs J C, et al. First observation of edge localized modes mitigation with resonant and nonresonant magnetic perturbations in ASDEX upgrade[J]. Physical review letters, 2011, 106(22): 225004.
- [4] Chapman I T, Kirk A, Akers R J, et al. Assessing the merits of resonant magnetic perturbations with different toroidal mode numbers for controlling edge localised modes[J]. Nuclear Fusion, 2014, 54(12): 123003.
- [5] Jakubowski M W, Evans T E, Fenstermacher M E, et al. Overview of the results on divertor heat loads in RMP controlled H-mode plasmas on DIII-D[J]. Nuclear fusion, 2009, 49(9): 095013.
- [6] Jeon Y M, Park J K, Yoon S W, et al. Suppression of edge localized modes in high-confinement KSTAR plasmas by nonaxisymmetric magnetic perturbations[J]. Physical review letters, 2012, 109(3): 035004.
- [7] Suttrop W, Eich T, Fuchs J C, et al. First observation of edge localized modes mitigation with resonant and nonresonant magnetic perturbations in ASDEX upgrade[J]. Physical review letters, 2011, 106(22): 225004.
- [8] Kirk A, Liu Y, Nardon E, et al. Magnetic perturbation experiments on MAST L-and H-mode plasmas using internal coils[J]. Plasma Physics and Controlled Fusion, 2011, 53(6): 065011.
- [9] Liu Y, Kirk A, Gribov Y, et al. Modelling of plasma response to resonant magnetic perturbation fields in MAST and ITER[J]. Nuclear Fusion, 2011, 51(8): 083002.
- [10] Jia M, Loarte A, Sun Y, et al. Integrated ELM and divertor power flux control using RMPs with low input torque in EAST in support of the ITER research plan[J]. Nuclear Fusion, 2021, 61(10): 106023.
- [11] Liu Y Q, Bondeson A, Fransson C M, et al. Feedback stabilization of nonaxisymmetric resistive wall modes in tokamaks. I. Electromagnetic model[J].
- [12] Bozhnikov S A, Jakubowski M W, Niemann H, et al. Effect of error field correction coils on W7-X limiter loads[J]. Nuclear Fusion, 2017, 57(12): 126030.
- [13] Li L, Liu Y Q, Liang Y, et al. Screening of external magnetic perturbation fields due to sheared plasma flow[J]. Nuclear fusion, 2016, 56(9): 092008.
- [14] Li L, Liu Y Q, Loarte A, et al. Modeling 3D plasma boundary corrugation and tailoring toroidal torque profiles with resonant magnetic perturbation fields in ITER[J]. Nuclear Fusion, 2019, 59(9): 096038.